EFFECT OF GEOMETRIC IMPERFECTIONS ON SHELLS CONVEYING FLUID

Marco Amabili
Dipartimento di Ingegneria Industriale, Università di Parma, Parma, Italy

Kostas Karagiozis
Mechanical Science and Engineering Department, University of Illinois, Urbana, Illinois, U.S.A

Michael P.Païdoussis
Mechanical Engineering Department, McGill University, Montreal, Quebéc, Canada

ABSTRACT

Circular cylindrical shells conveying subsonic flow are addressed in the present study; they lose stability by divergence when the flow speed reaches a critical value. The divergence is strongly subcritical, becoming supercritical for larger amplitudes. In the present paper, a nonlinear theoretical model for shells with large displacements and a linear flow theory are coupled. The effects of initial geometrical shell imperfections are also investigated. Numerical and experimental results for aluminium shells subjected to internal fluid flow are presented, showing an excellent agreement between theory and experiments.

1. INTRODUCTION

Thin-walled circular cylindrical shell structures conveying fluid may be found in many engineering and biomechanical systems. There are many applications of great interest in which shells are subjected to incompressible subsonic flows. For example, thin cylindrical shells are used as thermal shields in nuclear reactors and heat shields in aircraft engines; they may also be found in jet pumps and heat exchangers; they are used as storage tanks and thin-walled piping for aerospace vehicles. Furthermore, in biomechanics, veins, pulmonary passages and urinary systems may be modelled as shells conveying fluid.

Circular cylindrical shells containing subsonic flow are addressed in this study; they lose stability by divergence (which is a static pitchfork bifurcation of the equilibrium, exactly the same as buckling) when the flow speed reaches a critical value. According to the few available studies [see Amabili et al. (2003)], the divergence is strongly subcritical, becoming supercritical at larger amplitudes. It is very interesting to observe that the shell system has two or more stable solutions concurrently, related to divergence in the first mode or a combination of the first and second longitudinal modes, much before the onset of the pitchfork bifurcation. This means that the shell, if perturbed from the initial configuration, may be subjected to severe deformations causing failure at flows much smaller than the critical velocity predicted by the linear threshold. This indicates the necessity of using a nonlinear shell theory for engineering design.

The literature on the dynamic stability of circular cylindrical shells in the presence of internal or external axial flows is quite extensive. The effects of an internal flow have been studied, for example, by Païdoussis and Denise (1972), Weaver and Unny (1973), Païdoussis (1998), Amabili and Garziera (2002a, b) and others. As shown by Païdoussis (1998) and Amabili and Garziera (2002), the effect of viscous forces is not particularly large for short shells subjected to internal flow. In the previously mentioned studies, linear shell theories and potential flow theory are used.

The studies developed in the past for the stability of circular cylindrical shells in axial flow do not agree sufficiently well with experimental results, as pointed out by Horn et al. (1974). In particular, for subsonic Mach numbers, highly divergent and catastrophic instabilities have been encountered experimentally for clamped-clamped copper shells excited by a fully developed turbulent flow.

The problem was solved for the first time by Amabili, Pellicano and Païdoussis (1999), who discovered the post-divergence strongly subcritical behaviour. They used Donnell's nonlinear shallow-shell theory and a base of seven natural modes to study in depth the nonlinear vibrations and stability of simply supported circular cylindrical shells conveying or immersed in subsonic flow. Karagiozis et al. (2008) developed a nonlinear model for shells with clamped ends and successfully compared theoretical results with experimental data. Experiments, confirming the calculations, were previously performed by Karagiozis (2006) and Karagiozis et al. (2005).

For the interested reader a detailed review of linear and nonlinear studies is given in Amabili et al. (2003) and Paidoussis (2003).

The novel features of the present study are: (i) the introduction of geometric imperfections, which give fundamental qualitative and quantitative differences in behaviour *vis-à-vis* a perfect shell; (ii) the use of

more refined nonlinear shell theories retaining in-plane displacements (without the introduction of a potential stress function), i.e. Donnell's theory with in-plane displacements and the Sanders-Koiter theory; (iii) the introduction of non-classical boundary conditions that allows the exact simulation of the experimental conditions described in Karagiozis et al. (2005, 2008).

2. NONLINEAR THEORETICAL MODEL

The system under consideration is a thin circular cylindrical shell, of length *L*, mean radius *R*, and thickness *h*, as shown in Figure 1. The shell is assumed to be homogeneous and isotropic with Young's modulus *E* and Poisson ratio *ν*. A Cartesian coordinate system is assumed, with its origin attached at one end of the shell, and the middle surface displacements in the axial, circumferential and radial directions are denoted by *u*, *v*, and *w*, respectively.

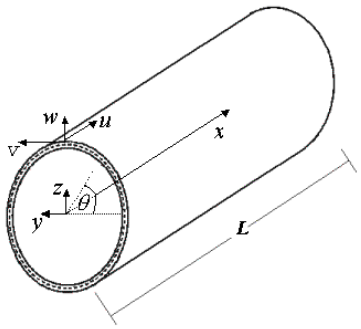

Figure 1: *Shell geometry*.

Two different nonlinear shell theories are employed to describe the shell motions. The first model used the nonlinear Donnell theory for shallow shells with in-plane displacements accounted for in the equations of motion. The second model used a more elaborate scheme employing the Sanders-Koiter nonlinear theory for shells.

The equation of motion is derived using the Lagrange equation in a variational approach. The final expression for the Lagrange equation is given by

$$\frac{\mathrm{d}}{\mathrm{d}t}\left[\frac{\partial(T_S+T_F)}{\partial\dot{q}_j}\right]-2\frac{\partial E_G}{\partial q_j}+\frac{\partial(U_S+V_F)}{\partial q_j}=Q_j\,, \quad (1)$$

where, $j=1,\ldots,\bar{N}$, T_S and V_S are the kinetic and potential energies of the structure including the effect of the boundary conditions, T_F and V_F are the kinetic and potential energies of the fluid, E_G is the gyroscopic energy associated with the flow potential, Q_j are the generalized external forces and q_j the generalized coordinates. To obtain the expressions for the kinetic and potential structural energy, a suitable nonlinear model is chosen to describe the relationships between displacements, strains and stresses.

2.1 Structural model

For a homogeneous and isotropic material ($\sigma_z=0$, case of plane stress) the relationship between stress and strains is given by

$$\sigma_x=\frac{E}{1-\nu^2}\left(\varepsilon_x+\nu\,\varepsilon_\theta\right),\ \ \sigma_\theta=\frac{E}{1-\nu^2}\left(\varepsilon_\theta+\nu\,\varepsilon_x\right),$$
$$\tau_{x\theta}=\frac{E}{2(1+\nu)}\gamma_{x\theta}\,. \quad (2)$$

According to classical shell theories [see Amabili (2003)], the strain components ε_x, ε_θ and $\gamma_{x\theta}$ at an arbitrary point of the shell are related to the middle surface strains $\varepsilon_{x,0}$, $\varepsilon_{\theta,0}$ and $\gamma_{x\theta,0}$ and to the changes in the curvature and torsion of the middle surface k_x, k_θ and $k_{x\theta}$ by the following three relationships: $\varepsilon_x=\varepsilon_{x,0}+z\,k_x$, $\varepsilon_\theta=\varepsilon_{\theta,0}+z\,k_\theta$, and $\gamma_{x\theta}=\gamma_{x\theta,0}+z\,k_{x\theta}$, where z is the distance of the arbitrary point of the shell from the middle surface. Therefore the expression for the potential energy of the structure is given by

$$U_S=U_{\text{shell}}+U_{\text{spring}}\,, \quad (3)$$

where U_{shell} is the strain energy of the shell and U_{spring} is the strain energy associated with the boundary conditions. Special attention on the theoretical representation of the boundary conditions applied at the shell edges is given in the following subsection. The final expression for the shell strain energy, including the effect of membrane, bending and the interaction of the two, is given by

$$U_{shell}=\frac{1}{2}\frac{E\,h}{1-\nu^2}\int_0^{2\pi}\int_0^{L}\Big(\varepsilon_{x,0}^2+\varepsilon_{\theta,0}^2+2\nu\,\varepsilon_{x,0}\,\varepsilon_{\theta,0}+$$
$$\frac{1-\nu}{2}\gamma_{x\theta,0}^2\Big)\mathrm{d}\,x\,R\,\mathrm{d}\,\theta+\frac{1}{2}\frac{E\,h^3}{12\left(1-\nu^2\right)}\int_0^{2\pi}\int_0^{L}\Big(k_x^2+$$
$$k_\theta^2+2\nu\,k_x\,k_\theta+\frac{1-\nu}{2}k_{x\theta}^2\Big)\mathrm{d}\,x\,R\,\mathrm{d}\,\theta+\frac{E\,h^3}{12R\left(1-\nu^2\right)}\times$$
$$\int_0^{2\pi}\int_0^{L}\Big(\varepsilon_{x,0}\,k_x+\varepsilon_{\theta,0}\,k_\theta+\nu\,\varepsilon_{x,0}\,k_\theta+\nu\,\varepsilon_{\theta,0}\,k_x+$$
$$\frac{1-\nu}{2}\gamma_{x\theta,0}\,k_{x\theta}\Big)\mathrm{d}\,x\,R\,\mathrm{d}\,\theta+O(h^4)\,. \quad (4)$$

Neglecting rotary inertia but retaining in-plane inertia, the kinetic energy T_S of a circular cylindrical

shell is given by

$$T_S = \frac{1}{2}\rho_S h \int_0^{2\pi}\int_0^{L}\left(\dot{u}^2+\dot{v}^2+\dot{w}^2\right)\mathrm{d}x R\,\mathrm{d}\theta, \qquad (5)$$

where ρ_S is the mass density of the shell.

The generalized forces Q_j are obtained by differentiation of the Rayleigh dissipation function and of the virtual work W done by external forces:

$$Q_j = -\frac{\partial F}{\partial \dot{q}_j}+\frac{\partial W}{\partial q_j}, \qquad (6)$$

where $\partial F/\partial \dot{q}_j = c_j \dot{q}_j$. The expressions for the Rayleigh dissipation function F, and the work done by external forces are explicitly given in Amabili (2003).

2.2 Boundary conditions

The following boundary conditions are imposed at the shell ends (see Figure 1):

$v = w = w_0 = 0$, $N_x = -k_a u$, $M_x = -k_r(\partial w/\partial x)$, at $x = 0, L$, (7)

where N_x is the axial load per unit length (around the circumference), M_x is the bending moment per unit length, k_a is stiffness per unit length of the elastic, distributed axial springs at $x = 0$ and L and k_r is the stiffness per unit length of the elastic, distributed rotational springs at $x = 0$ and L. Moreover, u, v and w must be continuous in θ. The last boundary condition accepts different values for the axial spring k_a thus simulating different experimental boundary conditions. For example, it produces boundary conditions from a case of zero moment ($M_x = 0$, unconstrained rotation) to a perfectly rotationally clamped shell ($\partial w/\partial x = 0$, obtained as limit for $k_r \to \infty$), according to the value of k_r. In the case of not very short thin shells, the axial spring k_a plays a much larger role than the rotational spring k_r.

2.3 Solution expansion

A base of shell displacements is used to discretize the system; the displacements u, v and w can be expanded by using the following expressions, which identically satisfy the boundary conditions:

$$u(x,\theta,t) = \sum_{m=1}^{M_1}\sum_{j=1}^{N}\left[u_{m,j,c}(t)\cos(j\theta)+u_{m,j,s}(t)\sin(j\theta)\right]\cos(\lambda_m x) + \sum_{m=1}^{M_2} u_{m,0}(t)\cos(\lambda_m x),$$

$$v(x,\theta,t) = \sum_{m=1}^{M_1}\sum_{j=1}^{N}\left[v_{m,j,c}(t)\sin(j\theta)+v_{m,j,s}(t)\cos(j\theta)\right]\sin(\lambda_m x),$$

$$w(x,\theta,t) = \sum_{m=1}^{M_1}\sum_{j=1}^{N}\left[w_{m,j,c}(t)\cos(j\theta)+w_{m,j,s}(t)\sin(j\theta)\right]\sin(\lambda_m x) + \sum_{m=1}^{M_2} w_{m,0}(t)\sin(\lambda_m x), \qquad (8)$$

where j is the number of circumferential waves, m is the number of longitudinal half-waves, $\lambda_m = m\pi/L$ and t is the time; $u_{m,j}(t)$, $v_{m,j}(t)$ and $w_{m,j}(t)$ are the generalized coordinates, which are unknown functions of t; the additional subscript c or s indicates whether the generalized coordinate is associated with a cosine or sine function in θ, except for v, for which the notation is reversed; no additional subscript is used for axisymmetric terms. The integers N, M_1 and M_2 must be selected with care in order to obtain an acceptable dimension of the nonlinear problem and the required accuracy.

Imperfections are expanded according to the following Fourier series,

$$w_0(x,\theta,t) = \sum_{m=1}^{\hat{M}}\sum_{j=0}^{\hat{N}}\left[A_{m,n}\cos(j\theta)+B_{m,n}\sin(j\theta)\right]\sin(m\pi x/L). \qquad (9)$$

2.4 Fluid-dynamics model

2.4.1 Fluid structure interaction

The shell is considered to be conveying incompressible fluid. Furthermore, it is assumed that the fluid is inviscid and isentropic and the flow is irrotational. Nonlinearities in the dynamic pressure and in the boundary conditions at the fluid-structure interface are neglected, because fluid movements of the order of the shell thickness may be considered to be small; and hence a linear formulation is quite reasonable [see Gonçalves and Batista (1988)]. In addition, pre-stress in the shell due to fluid weight (hydrostatic effect) is neglected. With these assumptions in mind, the fluid structure-interaction can be described by potential flow theory. The potential flow is comprised of two terms, one which is represented by the uniform axial undisturbed mean flow velocity, and the other one by the unsteady flow. The expression for the unsteady potential flow is obtained by solving the Laplace equation

$$\nabla^2\Phi = \frac{\partial^2\Phi}{\partial x^2}+\frac{\partial^2\Phi}{\partial r^2}+\frac{1}{r}\frac{\partial\Phi}{\partial r}+\frac{1}{r^2}\frac{\partial^2\Phi}{\partial\theta^2} = 0, \qquad (10)$$

where $\Phi(x,\theta,r,t)$ is the unsteady potential flow, r is the mean radius of the flow domain. Accordingly, the total perturbed pressure P acting on the fluid-shell interface is defined as the combination of the mean pressure $\overline{P}$ and the perturbation pressure p, i.e., $P = \overline{P} + p$. The perturbation pressure is found

using the linearized Bernoulli equation, yielding

$$p = -\rho_F \left(\partial\Phi/\partial t + U\,\partial\Phi/\partial x\right). \quad (11)$$

For this study, it is necessary to assume boundary conditions also beyond the shell extremities. Since any system is different, and since different inflow and outflow boundary conditions do not affect the results as greatly if they are taken sufficiently far away from the shell, simplified models can conveniently be introduced. The fluid domain is assumed to be a cylinder of infinite extent, within a periodically supported shell of infinite length so that it is possible to employ the method of separation of variables to obtain the velocity potential. The distance between periodic supports is *L*. This means that the shell radial displacement *w* is assumed to be a periodic function with main period 2*L*, and the same is satisfied by the velocity potential and the perturbation pressure.

If no cavitation occurs at the fluid-shell interface, the boundary condition expressing the contact between the shell wall and the flow is

$$\left(\frac{\partial \Phi}{\partial r}\right)_{r=R} = \left(\frac{\partial w}{\partial t} + U\frac{\partial w}{\partial x}\right). \quad (11)$$

Using the method of separation of variables, the final expression for the potential Φ is given by $\Phi = \sum_{m=1}^{M}\sum_{n=0}^{N} \frac{L}{m\pi}\frac{\mathrm{I}_n(m\pi r/L)}{\mathrm{I}'_n(m\pi R/L)}\left(\frac{\partial w_{m,n}}{\partial t} + U\frac{\partial w_{m,n}}{\partial x}\right)$, where I_n is the modified Bessel function of the first kind and of order *n*, and I'_n is the derivative of I_n with respect to the argument. Using the solution for Φ and equation (11), the perturbation pressure at the shell wall is

$$p = -\rho_F \sum_{m=1}^{M}\sum_{n=0}^{N} \frac{L}{m\pi}\frac{\mathrm{I}_n(m\pi R/L)}{\mathrm{I}'_n(m\pi R/L)}\left(\frac{\partial}{\partial t} + \frac{U\partial}{\partial x}\right)^2 w_{m,n}. \quad (12)$$

2.4.2 Energy associated with the flow

The total energy E_F, associated with the flow, can conveniently be divided into three terms with different contributions of time functions and their derivatives:

$$E_F = T_F + E_G - V_F. \quad (13)$$

The first and second of the three terms on the right-hand side can be identified as the kinetic and gyroscopic energies, respectively; an opposite sign is introduced for the potential energy V_F for convenience. The kinetic energy T_F of the fluid associated with the perturbation potential, by using the orthogonality of $\sin(m\pi x/L)$ in (0, *L*) and of $\cos(n\theta)$ in (0, 2π), is given by

$$T_F = \frac{1}{2}\rho_F \sum_{m=1}^{M}\sum_{n=0}^{N} \int_0^{2\pi}\int_0^{L} \frac{L}{m\pi}\frac{\mathrm{I}_n(m\pi R/L)}{\mathrm{I}'_n(m\pi R/L)}\dot{w}_{m,n}^2\,\mathrm{d}x R\,\mathrm{d}\theta. \quad (13)$$

An analogous expression for the kinetic energy of an external flow is given in Amabili (2003).

The potential energy V_F, by using the orthogonality of $\cos(m\pi x/L)$ in (0, *L*) and of $\cos(n\theta)$ in (0, 2π), is

$$V_F = -\frac{1}{2}\rho_F \sum_{m=1}^{M}\sum_{n=0}^{N} \int_0^{2\pi}\int_0^{L} \frac{L}{m\pi}\frac{\mathrm{I}_n(m\pi R/L)}{\mathrm{I}'_n(m\pi R/L)}U^2 \times \left(\frac{\partial w_{m,n}}{\partial x}\right)^2 \mathrm{d}x R\,\mathrm{d}\theta. \quad (14)$$

Equation (14) shows that V_F is negative, that is, the stiffness of the system is a decreasing function of *U*. This explains the shell instability at sufficiently high values of *U*.

The final expression for the gyroscopic energy E_G associated with the perturbation potential is

$$E_G = \frac{1}{2}\rho_F \sum_{m=1}^{M}\sum_{l=1}^{M}\sum_{n=0}^{N}\sum_{k=0}^{N} \int_0^{2\pi}\int_0^{L} \frac{U\,L}{m\pi}\frac{\mathrm{I}_n(m\pi R/L)}{\mathrm{I}'_n(m\pi R/L)} \times \left(\dot{w}_{m,n}\frac{\partial w_{l,k}}{\partial x} + \dot{w}_{l,k}\frac{\partial w_{m,n}}{\partial x}\right)\mathrm{d}x R\,\mathrm{d}\theta. \quad (15)$$

One can easily verify that E_G is globally zero in the case of harmonic vibrations. This proves that the system is conservative. In fact, no energy is dissipated; the fluid is assumed to be inviscid. Note that equation (15) expresses a particular coupling between modes through damping that is characteristic of gyroscopic systems; in this class of problems belong systems with mass transport. Additional simplifications into the derivation of the flow energy is given in Amabili et al . (2003).

The final expressions for the structural and flow energies along with the work done by external forces are substituted in the Lagrange equation (1) to obtain the equations of motion in the global coordinates.

3. COMPARISON WITH EXPERIMENTS

Experiments on stability of circular cylindrical shells conveying water flow were performed by Karagiozis et al. (2005, 2008). The water-flow (ρ_F =1000 kg/m^3) apparatus involves a modification of the vertical test-section of a water tunnel such that the flow from the upper part of a 203 mm diameter test-section is channeled into the test shell, which has a considerably smaller diameter (less than half). The test shell is surrounded by quiescent water, see Figure 2; in the tests, the pressure in that fluid region was higher than the pressure in the internally flowing fluid at mid-length of the shell, that is, $P_{\mathrm{ann}} > P_{\mathrm{inn}}$ at $x = L/2$. Thus, there was a net inward-acting pressure (negative pressure p_m). This was necessary to achieve flow-induced instability for some of the shells, because of the limited maximum

flow velocity attainable in the water tunnel. Experiments were conducted on aluminium shells glued to copper rings. The tested shells have the following dimensions and material properties: L=0.1225 m; R=0.041125 m; h=0.000137 m; ρ_S=2720 kg/m^3; ν = 0.38 and E = 70×10^9 Pa; the radius delimiting the still fluid domain is R_1 = 0.1015 m.

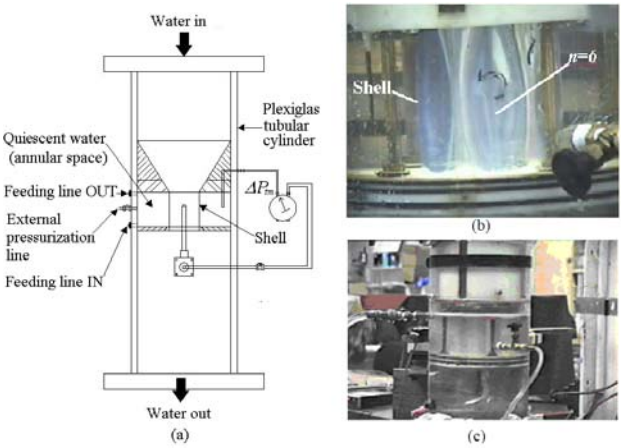

Figure 2: *Apparatus for water tunnel experiments.*

The rings sat on plastic supports in the test-section and were sealed with silicone rubber. Experimental boundary conditions lie between ideal simply supported and clamped ends, being closer to the simply supported ends. In particular, no axial constraint is present, so far as axisymmetric modes are concerned. A nondimensional fluid velocity V is introduced for convenience, defined as in Weaver and Unny (1973): $V = U / \left\{ (\pi^2 / L) \left[D / (\rho h) \right]^{1/2} \right\}$, with $D = E h^3 / \left[12(1-\nu^2) \right]$.

3.1 Nonlinear results

Figure 3 shows theoretical nonlinear results displaying a strong subcritical pitchfork bifurcation underlying the large hysteresis between the onset and cessation of instability. The shell displacement, divided by the shell thickness is plotted against the non-dimensional water velocity V for three different boundary conditions at the shell ends: (i) simply supported boundary conditions, (ii) distributed springs at x = 0 and L of stiffness k_a= 1×10^7 N/m^2 and k_r= 0.3×10^3 N/rad (thin line) and (iii) clamped edges for asymmetric modes simulated with k_a= 1×10^{11} N/m^2 and k_r= 1×10^6 N/rad. These results are for a perfect shell.

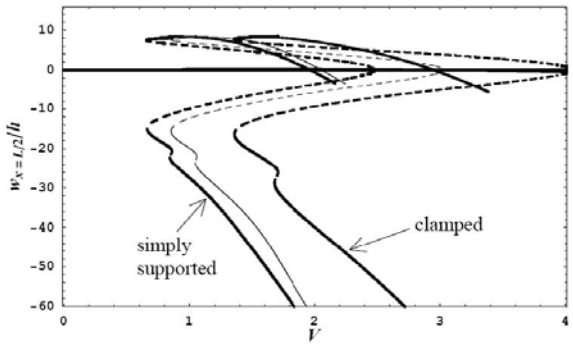

Figure 3: *Comparison of theoretical model with different boundary conditions for an aluminium shell with internal water flow n*=6, *transmural pressure* $\Delta P_{(x=L/2)} = 5.8$ kPa.

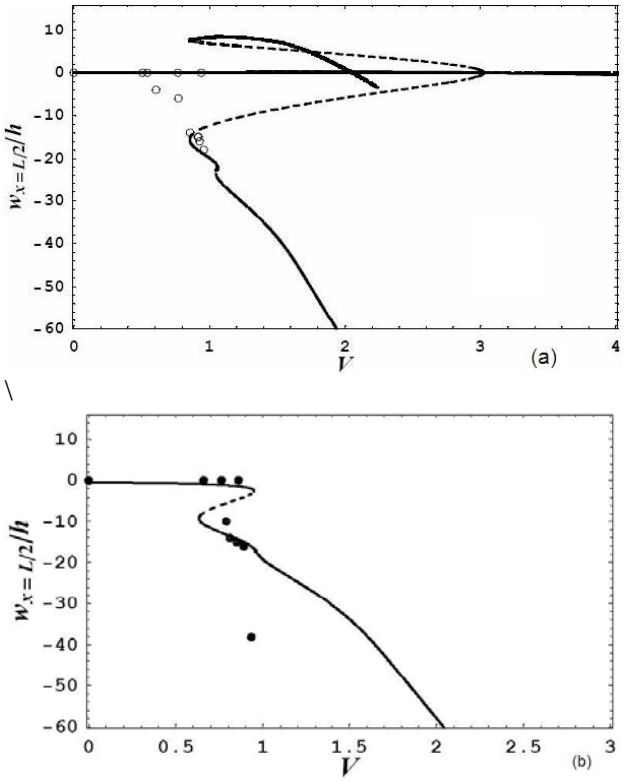

Figure 5: *Comparison of experimental and theoretical results including geometrical impterfections for an aluminium shell with n=6 and* $\Delta P_{(x=L/2)} = 5.8$ kPa. ——, *stable solutions;* – –, *unstable solutions. (a) Perfect shell model; (b) shell with initial imperfections (A1,n = -3.05h).*

Two representative sets of experimental results are shown in Figures 4(a,b); Fig. 4(a) shows results for a perfect shell and Fig.4(b) theoretical results including initial shell imperfections, along with experimental data. A very large difference is

observed between the instability point predicted by linear theory and the actual value under perturbations, showing that a nonlinear approach is absolutely necessary for a safe design of shells conveying flow.

4. CONCLUSIONS

A reasonably good agreement between experimental and theoretical results was obtained for shells with initial imperfections and mixed boundary conditions. Axisymmetric and asymmetric imperfections with a number of circumferential waves which is not a multiple of number of waves at instability play a small role. Calculations show the convergence of the solution and the accuracy of Donnell's theory retaining in-plane displacements for thin shells.

From the design point of view, this study shows that the critical flow velocity for shells cannot be predicted by a linear analysis, and that existing safety criteria may be inadequate, due to the subcritical bifurcation associated with loss of stability.

5. ACKNOWLEGMENTS

The authors would like to thank NSERC of Canada and FQRNT of Québec for their financial support.

6. REFERENCES

Amabili, M., 2003, Nonlinear vibrations of circular cylindrical shells with different boundary conditions. *AIAA Journal* **41**: 1119-1130.

Amabili,M, Garziera,R., 2002a, Vibrations of circular cylindrical shells with nonuniform constraints, elastic bed and added mass; Part II: shells containing or immersed in axial flow. *Journal of Fluids and Structures* **16:** 31-51.

Amabili,M, Garziera,R., 2002b, Vibrations of circular cylindrical shells with nonuniform constraints, elastic bed and added mass; Part III: shells containing or immersed in axial flow. *Journal of Fluids and Structures* **16:** 796-809.

Amabili, M., Païdoussis, M.P. 2003, Review of studies on geometrically nonlinear vibrations and dynamics of circular cylindrical shells and panels, with and without fluid-structure interaction. *Applied Mechanics Reviews* **56**: 349-381.

Amabili, M., Pellicano, F., M.P.Païdoussis, 1999, Nonlinear dynamics and stability of circular cylindrical shells containing flowing fluid. Part I: Stability. *Journal of Sound and Vibration* **225**: 655-699.

Gonçalves, P.B., Batista, R.C., 1988, Non-linear vibration analysis of fluid-filled cylindrical shells. *Journal of Sound and Vibration* **127**: 133-143.

Horn,W., Barr, G.W., Carter, L., Stearman, R.O., 1974, Recent contributions to experiments on cylindrical shell panel flutter. *AIAA Journal* **12:** 1481-1490.

Karagiozis, K.N., 2006, Experiments and theory on the nonlinear dynamics and stability of clamped shells subjected to axial fluid flow or harmonic excitation, Ph.D. Thesis, McGill University.

Karagiozis, K.N., Païdoussis, M.P., Misra, A.K., Grinevich, E., 2005, An experimental study of the nonlinear dynamics of cylindrical shells with clamped ends subjected to axial flow. *Journal of Fluids and Structures* **20**: 801-816.

Karagiozis,K.N., Païdoussis, M.P., Amabili,M., Misra, A.K., 2008, Nonlinear stability of cylindrical shells subjected to axial flow: Theory and experiments. *Journal of Sound and Vibration*, **309**: 637-676.

Païdoussis, M.P., 1998, *Fluid-Structure Interaction: Slender Structures and Axial Flow*, Vol. 1, London: Academic Press.

Païdoussis, M.P., 2004, *Fluid-Structure Interactions: Slender Structures and Axial Flow*, Vol. 2, Elsevier Academic Press, London, UK.

Païdoussis, M.P., Denise, J.P., 1972, Flutter of thin cylindrical shells conveying fluid. *Journal of Sound and Vibration* **20**: 9-26.

Weaver, D.S., Unny, T.E., 1973, On the dynamic stability of fluid-conveying pipes. *Journal of Applied Mechanics* **40:** 48-52.